Iterative Tikhonov regularization for the Cauchy problem for the Helmholtz equation

Fredrik Berntsson, Vladimir Kozlov, L. Mpinganzima and Bengt-Ove Turesson

Journal Article

Iterative Tikhonov Regularization for the Cauchy Problem for the Helmholtz Equation

F. Berntsson[a*], V.A. Kozlov[a], L. Mpinganzima[b] and B.O. Turesson[a]

November 17, 2016

Abstract

The Cauchy problem for the Helmholtz equation appears in various applications. The problem is severely ill-posed and regualrization is needed to obtain accurate solutions. We start from a formulation of this problem as an operator equation on the boundary of the domain and consider the equation in $(H^{1/2})^*$ spaces. By introducing an artificial boundary in the interior of the domain we obtain an inner product for this Hilbert space in terms of a quadratic form associated with the Helmholtz equation; perturbed by an integral over the artificial boundary. The perturbation guarantees positivity property of the quadratic form. This inner product allows an efficient evaluation of the adjoint operator in terms of solution of a well-posed boundary value problem for the Helmholtz equation with transmission boundary conditions on the artificial boundary.

In an earlier paper we showed how to take advantage of this framework to implement the conjugate gradient method for solving the Cauchy problem. In this work we instead use the Conjugate gradient method for minimizing a Tikhonov functional. The added penalty term regularize the problem and gives us a regularization parameter that can be used to easily control the stability of the numerical solution with respect to measurement errors in the data. Numerical tests show that the proposed algorithm works well.

Key words. Helmholtz equation; Cauchy problem; Adjoint Method; Inverse problem; Ill–posed problem; Tikhonov Regularization

1 Introduction

The Helmholtz equation arises in a wide range of applications related to acoustic and electromagnetic waves. Depending on the type of the boundary conditions, it appears in inverse problems for the determination of acoustic cavities [5], the detection of the source of acoustical noise [6, 7], the description of underwater

[**] Corresponding author. Email: fredrik.berntsson@liu.se. [a]*Department of Mathematics, Linköping University, SE-581 83 Linköping, Sweden* [b]*Department of Applied Mathematics, University of Rwanda, P.O. Box 117 Butare, Rwanda*

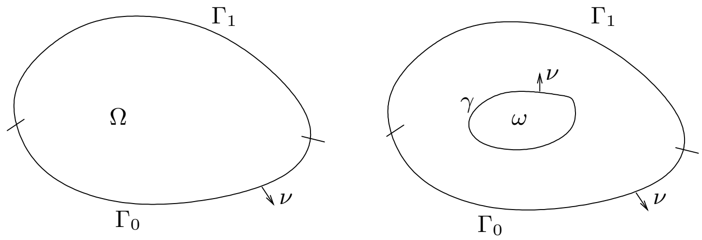

Figure 1: Description of the domain considered in this paper with a boundary Γ divided into two parts Γ_0 and Γ_1. On the right, an interior boundary γ_i has been introduced.

waves [10], the determination of the radiation field surrounding a source of radiation [24], and the localization of a tumor in a human body [26].

We consider the inverse problem of reconstructing the acoustic or electromagnetic field from inexact data given only on an open part of the boundary of a given domain. The governing equation for such a problem is the Helmholtz equation. In order to formulate the problem, we let Ω be a bounded domain in $\mathbb{R}^d$ with a Lipschitz boundary Γ divided into two disjoint parts Γ_0 and Γ_1 such that $\overline{\Gamma}_0 \cap \overline{\Gamma}_1$ is Lipschitz; see Figure 1.

The Cauchy data ϕ and ζ are only known on Γ_0, possibly with a certain noise level. We can thus formulate the problem as follows:

$$\begin{cases} \Delta u + k^2 u = 0 & \text{in} \quad \Omega, \\ u = \phi & \text{on} \quad \Gamma_0, \\ \partial_\nu u = \zeta & \text{on} \quad \Gamma_0, \end{cases} \tag{1.1}$$

where the wave number k is a positive real number, ν is the outward unit normal of the boundary Γ, and ∂_ν denotes the outward normal derivative. This is the Cauchy problem for the Helmholtz equation and it is severely ill–posed [9, 17, 20]. Hence, regularization is needed in order to solve the problem accurately. Different regularization methods have been suggested by various authors. We mention for instance the potential function method [27], the modified Tikhonov regularization method [9, 23], the truncation method [22], the method of approximate solutions [24], the wavelet moment method [1], the conjugate gradient methods with the boundary element method [16, 18], and the alternating boundary element method [17].

By taking advantage of the linearity of the equation (1.1) we can, e.g., set $\phi = 0$ and consider the following well-posed problem: Find $u \in H^1(\Omega)$ such that

$$\begin{cases} \Delta u + k^2 u = 0 & \text{in} \quad \Omega, \\ u = 0 & \text{on} \quad \Gamma_0, \\ \partial_\nu u = \eta & \text{on} \quad \Gamma_1, \end{cases} \tag{1.2}$$

where we have imposed Neumann conditions on Γ_1 and zero Dirichlet conditions on Γ_0. Using the above well-posed problem we define an operator

$$K\eta = \partial_\nu u|_{\Gamma_0}, \tag{1.3}$$

and we have effectively reformulated the Cauchy problem (1.2) as a linear operator equation $K\eta = \zeta$. The problem with such an approach is that the formulation (1.2) can have non-zero solutions even for $\eta = 0$, or the solution in the interior may have a large norm due to clustering of eigenvalues near k^2.

The operator equation (1.3) can be considered in weighted L^2 spaces, see [12], or using $H^{1/2}$ spaces. We consider the second option and the space for η is $H^{1/2}(\Gamma_1)^*$. Then the solution u belongs to $H^1(\Omega)$ and $K\eta$ lies in $H^{1/2}(\Gamma_0)^*$. Despite the fact that both spaces are Hilbert it is problematic to find an expression for the adjoint K^* in terms suitable for applications. It is important to find inner products for these spaces that allows the efficient evaluation of the adjoint operator.

In the case $k = 0$, i.e. the Laplace equation, we can use an equivalent Hilbert norm in $H^{1/2}(\Gamma_1)^*$,

$$\|\eta\|_{H^{1/2}(\Gamma_1)^*} = (\int_\Omega |\nabla u|^2 dx)^{1/2}, \tag{1.4}$$

where u is harmonic and $u = 0$ on Γ_0 and $u = \eta$ on Γ_1. The adjoint operator, with respect to the corresponding inner product, can be expressed through the solution of a boundary value problem for the Laplace equation. For the construction of the adjoint it is important to note that (1.4) is the bilinear form corresponding to the differential operator in (1.2) for $k=0$.

If $k \neq 0$ then the bilinear form corresponding to (1.2) may change sign. In [3, 2] we have suggested to use instead,

$$\int_\Omega (|\nabla u|^2 - k^2u^2)^2 dx + \mu \int_\gamma u^2 ds, \tag{1.5}$$

where γ is a surface in $\bar{\Omega}$ and μ is a positive constant. If γ and μ are chosen so that the form (1.5) is positive for $u \neq 0$ then the adjoint, with respect to the corresponding inner product, could also be defined in terms of a boundary value problem for the Helmholtz operator with suitable transmission conditions on γ.

The alternating iterative algorithm for the Cauchy problem for the Laplace equation, suggested by the authors in [14, 13], consists of solving two related Neumann-Dirichlet problems in sequence. The alternating algorithm can be seen as solving the operator equation (1.3) by the Landweber method and the two mixed Dirichlet-Neumann problems can be viewed as the application of either the operator K or its adjoint K^*. It has been shown in [3, Section 1.3] that the alternating algorithm does not always converge for large wave numbers k^2 in the Helmholtz equation. This is due to the fact that for large k^2 a certain quadratic form related to the Helmholtz equation fails to be positive definite.

In [3] we proposed a modification of the alternating algorithm, for the case $k \neq 0$, by introducing an interior artificial boundary γ and a positive parameter

μ. It was shown that by making an appropriate choice of γ and using a large enough number μ we can guarantee positivity of the quadratic form (1.5). For this case it was also shown that that the modified algorithm is convergent, but the convergence was slow. However, since the quadratic form associated with the problem is positive, we can introduce an inner product, as discussed above, that gives us a natural framwork that can be used to implement more sophisticated iterative methods. This was done in [2], where we showed that the conjugate gradient method can used for solving the Cauchy problem efficiently. Since the conjugate gradient iterations have a regularizing effect (see [8]) we could also solve the problem with noisy data.

An important advantage of the proposed algorithms is that they can be readily applied to more general problems. First we can treat more general second order elliptic equations in divergence form with variable coefficients, i.e.

$$\nabla \cdot (A(x)\nabla u(x)) + k(x)u(x) = 0, \quad \text{in } \Omega,$$

and

$$u = f, \quad \nu \cdot (A(x)\nabla u(x)) = \psi, \quad \text{on } \Gamma_0,$$

where A is a bounded matrix-function with variable coefficients and k is a bounded measurable function. Secondly, we can reconstruct elastic oscillations, with a fixed frequency, in non-homogeneous and non-isotrophic media by boundary measurements, i.e.

$$\sum_{j=1}^{3} \frac{\partial}{\partial x_j} \sigma_{ij}(u) + \rho(x) k^2 u_i = 0, \quad \text{in } \Omega, \quad i = 1, 2, 3,$$

and

$$u = \phi, \quad \nu \cdot \sigma = \Psi, \quad \text{on } \Gamma_0,$$

where σ is the stress tensor,

$$\sigma_{ij} = \frac{1}{2} \sum_{k,\ell=1}^{3} A_{ij}^{k\ell}(x) \left(\frac{\partial u_k}{\partial x_\ell} + \frac{\partial u_\ell}{\partial x_k} \right),$$

where $A_{ij}^{k\ell}$ and ρ are space dependent functions, and $u = (u_1, u_2, u_3)$ is the displacement vector.

The paper is organized as follows: In Section 2 we introduce our modified operator equation, inner products, and the adjoint operator. In Section 3 we introduce the Tikhonov functional and explain how to implement the conjugate gradient method for finding minimizing the functional. In Section 4 we present a simple test problem and give the details of our finite difference discretization. We also present numerical results that demonstrates that the algorithm works well and accurate solutions can be found. Finally, in Section 5, we draw some conclusions and give directions for future research regarding the method.

2 A Modified Operator Equation and Weak Solutions

In order to introduce a modified operator equation we first introduce an interior boundary γ as follows. Let ω be an open subset of Ω with a Lipschitz boundary γ such that its closure $\bar{\omega} \subset \Omega$. We denote the boundary $\partial\omega$ by γ; see Figure 1. For a function u, defined in Ω, we denote by $[u]$ and $[\partial_\nu u]$ the jump of the function u, and the jump of the normal derivative $\partial_\nu u$ across γ, respectively.

The modified operator equation is introduced as follows. Pick a positive number μ and consider the following problem: Find $u \in H^1(\Omega \backslash \gamma)$ such that

$$\begin{cases} \Delta u + k^2 u = 0 & \text{in} \quad \Omega\backslash\gamma, \\ u = 0 & \text{on} \quad \Gamma_0, \\ \partial_\nu u = \eta & \text{on} \quad \Gamma_1, \\ [\partial_\nu u] + \mu u = \xi & \text{on} \quad \gamma, \\ [u] = 0 & \text{on} \quad \gamma. \end{cases} \tag{2.6}$$

Using the above boundary value problem we define an operator N, analogous to (1.3), by

$$N(\eta, \xi) = \partial_\nu u|_{\Gamma_0}, \tag{2.7}$$

where u solves (2.6). Then the operator equation $N(\eta, \xi) = \zeta$ will deliver the solution to the problem (1.1), with $\phi = 0$.

The bilinear form associated with the the Helmholtz equation, the interior boundary, and the number $\mu > 0$, is

$$a_\mu(u, v) = \int_{\Omega\backslash\gamma} \big(\nabla u \cdot \nabla v - k^2 uv\big)\, dx + \mu \int_\gamma uv\, dS, \qquad \text{for } u, v \in H^1(\Omega). \tag{2.8}$$

In our previous work [3] we demonstrated that it is always possible to chose γ and μ such that

$$a_\mu(u, u) > 0, \qquad \text{for } u \neq 0,\, u \in H^1(\Omega). \tag{2.9}$$

This means that the bilinear form defines an inner product on $H^1(\Omega)$. The corresponding norm is defined by $\|u\|_\mu = a_\mu(u, u)^{1/2}$, for $u \in H^1(\Omega)$.

Definition 2.1 *Let $\eta \in H^{1/2}(\Gamma_1)^*$, and $\xi \in H^{1/2}(\gamma)^*$. A function $u \in H^1(\Omega)$ is a* weak solution *to problem (2.6) if it satisfies*

$$a_\mu(u, v) = \int_{\Gamma_1} \eta v\, dS + \int_\gamma \xi v\, dS,$$

for every function $v \in H^1(\Omega)$ such that $v = 0$ on $\Gamma_0\}$.

To show that the solution of the operator equation $N(\eta, \xi) = \zeta$, or more precisely the corresponding solution u to the problem (2.6), also delivers the solution to the problem (1.1), with $\phi = 0$, and thus also the solution to the original operator equation $K\eta = \zeta$ we do the following: Denote by u_1 the solution of (2.6) and by u_2 the solution of (1.1), with $\phi = 0$. The function $w = u_1 - u_2$ satisfies the homogeneous Cauchy problem for the Helmholtz operator in $\Omega\backslash\bar{\omega}$ and hence $w = 0$ in $\Omega\backslash\bar{\omega}$. This implies that $w = 0$ on $\gamma = \partial\omega$. Since the quadratic form is positive on ω this means that $w = 0$ in ω.

2.1 Inner products and the adjoint

The bilinear form is used to define inner products on the spaces $H^{1/2}(\Gamma_1)^* \times H^{1/2}(\gamma)^*$ and $H^{1/2}(\Gamma_0)^*$. For simplicity we denote the space $H^{1/2}(\Gamma_1)^* \times H^{1/2}(\gamma)^*$ by $(H^{1/2})^*$.

Definition 2.2 *Let $\chi_1 = (\eta_1, \xi_1)$ and $\chi_2 = (\eta_2, \xi_2)$ be two functions in $(H^{1/2})^*$. The inner product between χ_1 and χ_2 is*

$$(\chi_1, \chi_2)_{(H^{1/2})^*} = a_\mu(u_1, u_2),$$

where u_1 and u_2 satisfies the modified problem (2.6), with data (η_1, ξ_1) and (η_2, ξ_2), respectively.

In order to define an inner product on the space $H^{1/2}(\Gamma_0)^*$, we first introduce a second auxiliary problem: Find $u \in H^1\Omega$ such that

$$\begin{cases} \Delta u + k^2 u = 0 & \text{in} \quad \Omega\backslash\gamma, \\ \partial_\nu u = \zeta & \text{on} \quad \Gamma_0, \\ u = 0 & \text{on} \quad \Gamma_1 \cup \gamma. \end{cases} \tag{2.10}$$

Definition 2.3 *Let ζ_1 and ζ_2 be two functions in $H^{1/2}(\Gamma_0)^*$. The inner product between ζ_1 and ζ_2 is*

$$(\zeta_1, \zeta_2)_{H^{1/2}(\Gamma_0)^*} = a_\mu(u_1, u_2),$$

where u_1 and u_2 are solutions to (2.10), with data ζ_1 and ζ_2, respectively.

Finally the adjoint N^* is defined by

$$N^*\zeta = (\partial_\nu u|_{\Gamma_1}, ([\partial_\nu u] + \mu u)|_\gamma) = (\eta, \xi), \tag{2.11}$$

where u solves the problem (2.10) with $\partial_\nu u = \zeta$ on Γ_0.

3 Tikhonov Regularization

We recall that our goal is to solve the ill-posed operator equation

$$N\chi = \zeta, \qquad \chi = (\eta, \xi). \tag{3.12}$$

where N is defined by (2.7), and $N\chi$ can be evaluated by solving the well-posed problem (2.6) with data $\chi = (\eta, \xi)$. Note that, as explained previously, we have a natural framwork with a scalar product that allows us to define an adjoint N^* that can be evaluated by solving the well-posed problem (2.6) with appropriate data.

We propose to use Tikhonov regularization[21, 28], i.e. to find $\chi \in (H^{1/2})^*$ that minimizes the Tikhonov functional:

$$\mathcal{J}_\lambda(\chi) = \|N\chi - \zeta\|^2_{H^{1/2}(\Gamma_0)^*} + \lambda^2 \|\chi\|^2_{(H^{1/2})^*}, \tag{3.13}$$

where $\lambda > 0$ is the regularization parameter. The Tikhonov functional represents a compromise between minimizing the residual $\|N\chi - \zeta\|_{H^{1/2}(\Gamma_0)^*}$ and enforcing stability, i.e., keeping the solution norm $\|\chi\|_{(H^{1/2})^*}$ small.

In order to obtain high-quality solutions a good value for the regularization parameter λ is needed. If the noise level in the right-hand side is known then the *discrepancy principle* by Morozov [8, 19] picks a value λ such that the norm of the residual is of the same magnitude as the noise. The discrepancy principle is known to work well. In the case when it is difficult to accurately estimate the magnitude of the noise, we can instead use the L-curve criterion, originally introduced by Lawson and Hanson [15], see also [8, 11]. The L-curve is a plot of the norm of the residual versus the norm of the solution, which can be seen as a way of visualizing the trade-off between stability and keeping the residual small, and often leads to good regularization parameters in practice.

The normal equations that correspond to the minimization problem (3.13) are

$$N^* N\chi + \lambda^2 \chi = N^* \zeta. \tag{3.14}$$

For a given value of λ, this represents a well-posed operator equation, where the operator is self-adjoint and positive definite.

3.1 The conjugate gradient methods

The conjugate gradient method[25] (see also [8]) is the default choice when dealing with self-adjoint and positive definite equations. In this section, we describe the iterative procedure obtained when applying the conjugate gradient method to the normal equations (3.14).

Initially pick a starting guess $\chi_0 = (\eta_0, \xi_0) \in (H^{1/2})^*$, i.e. the normal derivative $\partial_\nu u$ on Γ_1 and the jump $[\partial_\nu u] + \mu u$ on the artificial inner boundary γ; see the problem (2.6). We also compute the initial residual by evaluating

$$d_0 = N^*(\zeta - N\chi_0) - \lambda^2 \chi_0, \tag{3.15}$$

where ζ is the known boundary data on Γ_0. Also set the initial search direction $p_0 = d_0$. Note that here we need to solve the boundary value problem (2.6) once, to evaluate $N\chi_0$, and the boundary value problem (2.10) twice, to evaluate $N^*\zeta$ and $N^*(N\chi_0)$.

Given χ_j, d_j, and p_j, the algorithm proceeds as follows: Evaluate

$$\zeta_j = Np_j, \tag{3.16}$$

by solving the boundary value problem (2.6). Compute the scalar

$$\alpha_j = \|d_j\|^2/(\|\zeta_j\|^2 + \lambda^2\|p_j\|^2), \tag{3.17}$$

and update the approximate solution and the residual by

$$\chi_{j+1} = \chi_j + \alpha_j p_j, \quad \text{and} \quad d_{j+1} = d_j - \alpha_j(N^*\zeta_j + \lambda^2 p_j), \tag{3.18}$$

where $N^*\zeta_j$ is evaluated by solving the boundary value problem (2.6), with data $\partial_\nu u = \zeta_j$ on Γ_0. Finally the new search direction is computed as

$$\beta_j = \|d_{j+1}\|^2/\|d_j\|^2, \quad \text{and} \quad p_{j+1} = d_j + \beta_j p_j. \tag{3.19}$$

In order to estimate the amount of work required for one iteration we note that the first step is to evaluate $\zeta_j = Np_j$. This means that we need to find the solution u_j of (2.6) with $p_j = (\eta_j, \xi_j)$ as data. The norm is then evaluated as $\|p_j\|^2 = a_\mu(u_j, u_j)$. So by solving (2.6) once we obtain both ζ_j and $\|p_j\|^2$. In order to update the residual d_j we then need to evaluate $N^*\zeta_j$, i.e. solve (2.10), with data ζ_j, to find the solution v_j. Thus, we get both the norm $\|\zeta_j\| = a_\mu(v_j, v_j)$ and the function $N^*\zeta_j$ by solving one boundary value problem.

In our implementation, we solve two more boundary value problems to compute $\|p_j\|$ and $\|d_j\|$ in each step of the algorithm. However, since the two problems are linear and d_j and p_j are obtained by linear combinations of functions, representing boundary data for (2.6) or (2.10) we could in principle obtain the solutions directly by linear combination of previously stored solutions; and thus two boundary value problems (one for N and one for N^*) is the minimum amount of work required to implement one conjugate gradient step.

4 Numerical Implementation and Tests

In order to conduct our tests we need to specify a geometry Ω, select the interior boundary γ, and also implement a finite difference method for solving the two well-posed problems that appear during the iterative process.

For our tests we chose a relatively simple geometry. Let L be a positive number and consider,

$$\Omega = (0,1)\times(0,L), \quad \text{with } \Gamma_0 = (0,1)\times\{0\} \text{ and } \quad \Gamma_1 = (0,1)\times\{L\}. \tag{4.20}$$

The geometry and boundary conditions are illustrated in Figure 2. Note that for our test geometry the two boundary parts Γ_0 and Γ_1 are disjoint. On the sides of the domain we set zero Dirichlet conditions, i.e.,

$$u(x,y) = 0 \quad \text{for } (x,y) \in \{0\}\times(0,L)\cup\{1\}\times(0,L). \tag{4.21}$$

In addition we pick a rectangular interior domain ω, with the same center of gravity as Ω and side lengths L_1 and L_2. The interior domain is also illustrated in Figure 2. The specific choice for the interior boundary is dependent on the first eigenvalue for the problem inside γ and for the problem outside γ are approximately equal; see [3] for further discussion about good choices of γ.

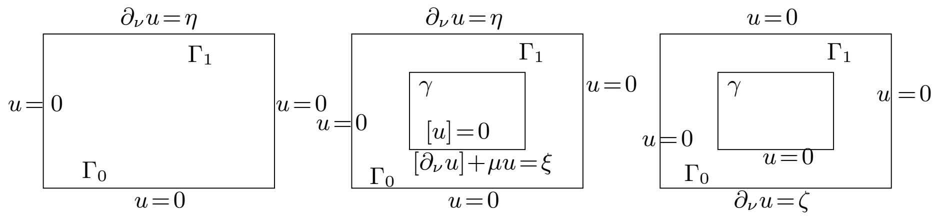

Figure 2: The domains and boudnary conditions for the numerical test problems. We display the settings for evaluating the operators K (left), N (middle) and N^* (right).

4.1 Numerical discretization

In order to implement numerical approximations of the operators K, N, and N^*, we need to solve the mixed boundary value problems (1.2), (2.6), and (2.10) respectively. In this section, we briefly give the details of our implementation of the finite difference method for solving these boundary value problems.

In our code, we discretize the domain Ω by choosing an equidistant grid $\{(x_i, y_j)\}$ of size $N \times M$. We use the same step size in the x- and y-directions and thus $M = LM$, and the step size is $h = N^{-1}$.

Let $u_{i,j}$ denote the discrete approximation to $u(x_i, y_j)$. At interior grid points the Helmholtz equation is approximated by

$$(4 - k^2h^2)u_{i,j} - u_{i-1,j} - u_{i+1,j} - u_{i,j-1} - u_{i,j+1} = 0. \tag{4.22}$$

At the boundaries corresponding to $x = 0$ and $x = 1$, the value of the function u is zero and the corresponding variables $u_{i,j}$ are explicitly set to zero. However, at the boundaries corresponding to $y = 0$ and $y = L$, we get different equations depending on the type of the boundary condition. Similarily Dirchlet conditions on Γ_0, Γ_1, or γ are dealt with by setting the corresponding variables $u_{i,j}$ to their respective values. Neumann boundary conditions are discretized using one sided second order accurate differences, i.e., at Γ_1, we obtain

$$(-3u_{i,M} + 4u_{i,M-1} - u_{i,M-2})(2h)^{-1} = \eta_i, \quad i = 0, \ldots, N, \tag{4.23}$$

and η_i is the prescribed Neumann data at $y = L$. Similar difference quotients are used to approximate Neumann boundary conditions at $y = 0$ and also for discretizing the jump $[\partial_\nu u]$ on the line segments making up the interior boudnary γ.

In our iterative solution method we need to repeatedly solve the well–posed problems that correspond to the operators N and N^*. In both cases, the finite difference method leeds to a linear system of equations $Ax = b$, where A is a large sparse MN by MN matrix, and b is a vector that contains the boundary data values.

In our experiments, these linear systems are solved using the LU decomposition of the sparse matrix A. Since the matrix A depends on the domain, the wave number k^2, the parameter μ, and the types of boundary conditions used, but not on the actual boundary data values, we can save the matrices A and their sparse LU decomposition between iterations. This significantly improves the computational speed.

The norms and the inner products introduced in Subsection 2.1 are also computed numerically by evaluating the intergrals that make up the bilinear form $a_\mu(u, v)$ (see (2.8)) on the grid using the trapezoidal rule. Note that the bilinear form involves an integral over the domain $\Omega\backslash\gamma$. The distinction between Ω and $\Omega\backslash\gamma$ is not important for the integration. However in the numerical implementation one-sided differences needs to be used for computing gradients near γ as the gradient may have a jump on γ.

4.2 Numerical Tests

In this section we present numerical experiments conducted with our algorithm in order to verify its validity.

In order to obtain suitable test problems for our algorithm we select the parameter $L = 0.2$, which determines the size of the domain Ω. Further the interior boundary γ is determined by the two parameters $L_1 = 0.20$ and $L_2 = 0.04$. The size of the computational grid used for the finite difference approximation is $N = 600$ and $M = 120$. Since the regularization parameter is the value λ we want to solve the modified normal equations to good accuracy. In our tests we stopped the CG iterations when the residual $\|d_k\|$ was below the tolerance 10^{-5}. This choice means we solve the normal equations with sufficient accuracy so that the main regularizing effect is due to the penalty term $\lambda^2\|\chi\|^2$ in the Tikhonov functional.

In order to create the numerical test problems we do the following: First select the function η and to be used as a boundary condition in (1.2), and also a wave-number k^2. Second we solve the problem to obtain the exaxt solution $u(x, y)$, and also compute the corresponding function $\zeta(x) = u_y(x, 0)$ to be used as a right hand side for the operator equation $K\eta = \zeta$. The problem is solved accurately enough so that with the data $u_y(x, 0) = \zeta$ and the solution η can be considered exact. In order to simulate measurement noise we added normally distributed random noise to the data ζ giving the noisy data vector ζ_m.

The starting guess χ_0 for the conjugate gradient iterations were created by setting $\eta_0 = \zeta_m$, and applying a simple smoothing filter. The initial data at the interior boundary, i.e. ξ_0, were obtained by solving the problem (1.2), using η_0 as data.

Example 4.1 The first test was conducted using $k^2 = 15.5$, $\mu = 2$, and a function η that was created using cubic spline interpolation and a small number of interpolation points. By solving the Helmholtz equation, i.e. the problem (1.2), we construct an exact solution u; from which we extract the boundary data ζ. Random noise with variance 10^{-2} was used to get the simulated measurements ζ_m. The exact solution $u(x, y)$, the boundary values $u_y(x, 1) = \eta$, and also the

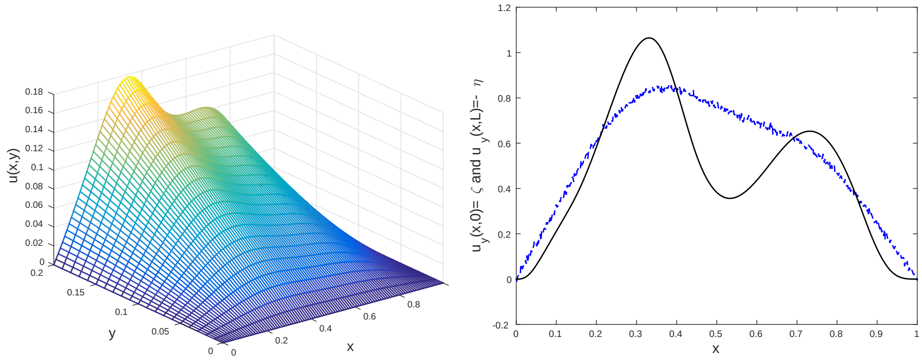

Figure 3: The exact solution $u(x, y)$ for Test 4.1 (left) and also the boundary data $u_y(x, 0) = \zeta(x)$ (right,blue curve) and $u_y(x, 1) = -\eta(x)$ (right,black dashed curve).

simulated measurements ζ_m are displayed in Figure 3. Note that the magnitude of the noise is rather large.

In order to find a regularized solution we selected $\lambda = 4 \cdot 10^{-3}$ and solved the normal equations using the conjugate gradient method to obtain the Tikhonov solution $(\eta^\lambda, \xi^\lambda)$. The results are displayed in Figure 4.

In order to illustrate the smoothing effects of the Tikhonov functional we also compute the solution for $\lambda = 4 \cdot 10^{-1}$. The results are shown in Figure 5.

It is crucial to pick a good value for the regularization parameter. In Figure 6 we use the L-curve to find a good value for λ.

Example 4.2 In our second test we increase the wave number to $k^2 = 25$. We also set $\mu = 5$ in order to make the quadratic form a_μ positive definite. In Figure 7 we display the results. The higher wave number does not generally make the problem more ill-posed. The noise level for the test was again a variance of 10^{-2} for the random simulated measurement errors. By picking an appropriate regularization parameter we manage to obtain a very good solution.

Example 4.3 In the third test we pick a simpler function $\eta(x)$ to use at the boundary $y = L$. With fewer complicated features to reconstruct we hope to obtain a more accurate solution. For this test we also used $k^2 = 25$. We also set $\mu = 5$. We also lowered the variance of the random noise to $5 \cdot 10^{-3}$.

In Figure 8 we display the results. With the simpler function η and the slightly lower noise level we manage to find a very good solution.

5 Concluding Remarks

It was proved in [3] that the alternating algorithm suggested by V.A. Kozlov and V.G. Maz'ya in [14] does not converge for large values of the wave number

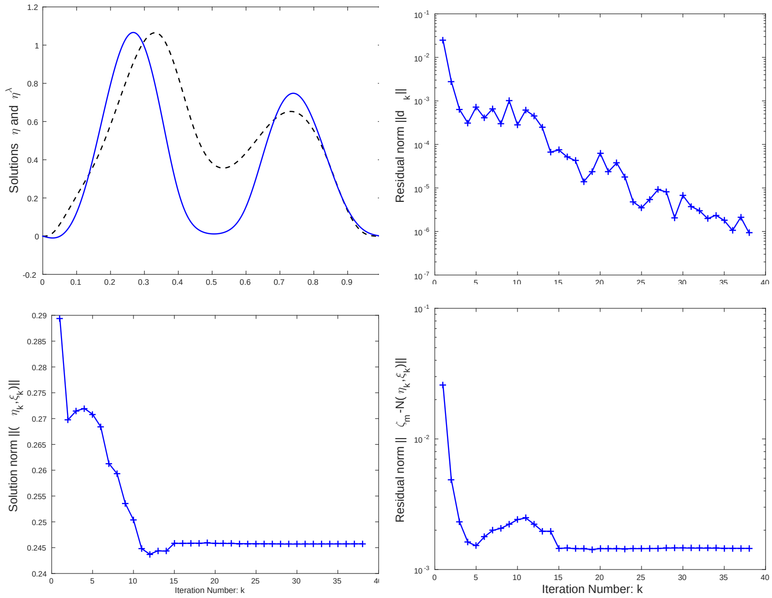

Figure 4: We display the Tikhonov solution η^λ, for $k^2 = 15.5$, $\mu = 2$, and $\lambda = 4 \cdot 10^{-2}$ (top left, blue curve). The Exact solution η (black, dashed) is also displayed. In addition we show the residual norm $\|d_k\|$ during the iterations (top,right). The stopping criteria is reached after $k = 37$ iterations. We also show the solution norm $\|(\eta_k, \xi_k)\|$ (lower,left) and the residual $\|\zeta_m - N(\eta_k, \xi_k)\|$ (lower,right) during the iterations.

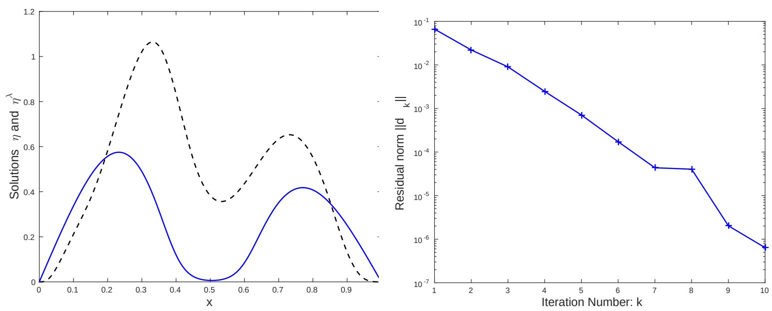

Figure 5: We display the Tikhonov solution η^λ, for $\lambda = 4 \cdot 10^{-1}$, (left, blue curve). The Exact solution η (black, dashed) is also displayed. For this case too much regularization is used the solution η^λ is too smooth. In addition we show the residual norm $\|d_k\|$ during the iterations (right). The stopping criteria is reached after $k = 9$ iterations.

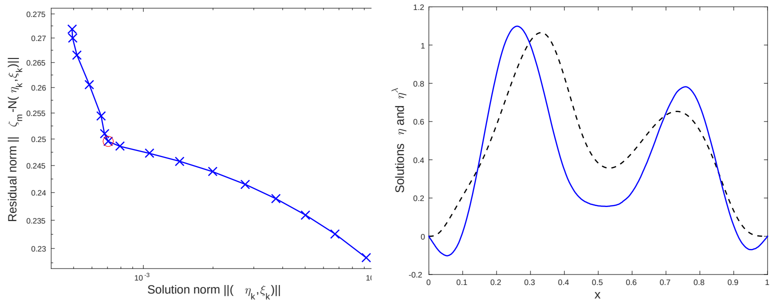

Figure 6: The L-curve (left) is a plot of residual norm $\|\zeta_m - N(\eta^\lambda, \xi^\lambda)\|$ versus the solution norm $\|(\eta^\lambda, \xi^\lambda)\|$ for a range of values λ. The corner of the curve is obtained for $\lambda = 2 \cdot 10^{-2}$ which represents a good compromise between accuracy and stability. The solution corresponding to $\lambda = 2 \cdot 10^{-2}$ is also displayed (right). For this case $k = 20$ iterations were used to calculate the solution.

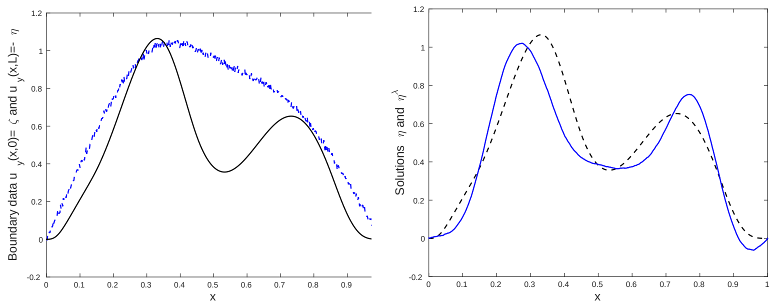

Figure 7: We display the noisy boundary data $\zeta_m(x)$ (left,blue curve) and $u_y(x, 1) = -\eta(x)$ (left,black dashed curve) for Test 4.2. We also show the Tikhonov solution η^λ, for $k^2 = 25$, $\mu = 5$, and $\lambda = 1 \cdot 10^{-2}$ (left, blue curve). The Exact solution η (black, dashed) is also displayed. For this case $k = 35$ iterations were used to solve the normal equations.

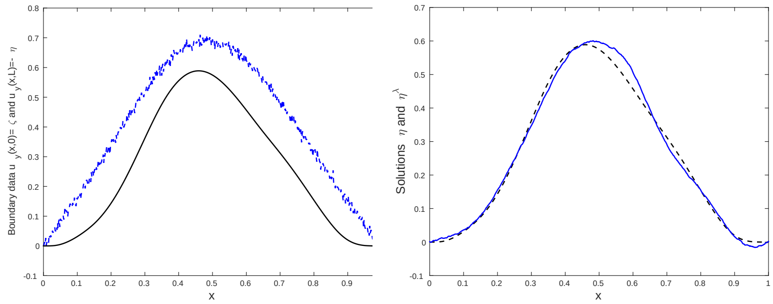

Figure 8: We display the noisy boundary data $\zeta_m(x)$ (left,blue curve) and $u_y(x,1) = -\eta(x)$ (left,black dashed curve) for Test 4.3. We also show the Tikhonov solution η^λ, for $k^2 = 25$, $\mu = 5$, and $\lambda = 1 \cdot 10^{-2}$ (left, blue curve). The Exact solution η (black, dashed) is also displayed. For this case $k = 17$ iterations were used to solve the normal equations.

k^2 in the Helmholtz equation. Instead we suggested a modification that includes an artificial interior boundary to restore convergence of the alternating iterative algorithm.

In [2] we noted that, if the modified alternating algorithm produces a convergent sequence, the bilinear form associated with the Helmholtz equation, the interior boundary γ and the parameter μ is coercive. This means that we can introduce a scalar product natural to the problem. We showed that we could rewrite the Cauchy problem as an operator equation and using the scalar product provided by the bilinear form we were able to derive an expression for the adjoint of the operator. As a result we demonstrated that the convergence of the method could be accelerated using conjugate gradient method for the normal equations.

The conjugate gradient iteration has regularizing properties but the algorithm turned out to be rather sensitive with respect to the number of iterations used; which acts as the regularization parameter. In this paper we proposed to use the conjugate gradient method for, instead, solving the normal equations that correspond to the minimization of the Tikhonov functional. This means we introduce a regularization parameter λ that can easily be changed to suit a specific problem. Our experiments demonstrate that the method works rather well and we obtain good solutions in a relatively low number of iterations. We also demonstrate that the L-curve technique can provide good regularization parameters when used together with our algorithm.

This paper represents an initial study and several aspects can be improved upon. Firstly the numerical tests are performed only with a simple geometry. In principle the method could deal with more complicated domains and equations. This is something we intend to explore in the future. Also, there are different approaches to restoring positive definiteness of the quadratic form. In [4] we proposed replacing Neumann conditions on Γ_0 and Γ_1 by Robin conditions.

This has the advantage that the function values on the interior boundary will not appear in the Tikhonov penalty term; which might lead to more accurate solutions on the part of Γ_1 that is "hidden" by γ. This is also something we intend to investigate in the future.

References

[1] W. Arendt and T. Regińska. An ill–posed boundary value problem for the helmholtz equation on lipschitz domains. *J. Inv. Ill–Posed Problems*, 17(7):703–711, 2009.

[2] F. Berntsson, V.A. Kozlov, L. Mpinganzima, and B.O. Turesson. An accelerated alternating procedure for the cauchy problem for the helmholtz equation. *Computers & Mathematics with Applications*, 68(1-2):44–60, 2014.

[3] F. Berntsson, V.A. Kozlov, L. Mpinganzima, and B.O. Turesson. An alternating iterative procedure for the cauchy problem for the helmholtz equation. *Inverse Problems in Science and Engineering*, 22(1):45–62, 2014.

[4] F. Berntsson, V.A. Kozlov, L. Mpinganzima, and B.O. Turesson. Robin–dirichlet algorithms for the cauchy problem for the helmholtz equation. *Submitted*, 2015.

[5] J.T. Chen and F.C. Wong. Dual formulation of multiple reciprocity method for the acoustic mode of a cavity with a thin partition. *Journal of Sound and Vibration*, 217(1):75–95, 1998.

[6] T. Delillo, V. Isakov, N. Valdivia, and L. Wang. The detection of the source of acoustical noise in two dimensions. *SIAM J. Appl. Math.*, 61(6):2104–2121, 2001.

[7] T. Delillo, V. Isakov, N. Valdivia, and L. Wang. The detection of surface vibrations from interior acoustical pressure. *Inverse Problems*, 19:507–524, 2003.

[8] H. Engl, M. Hanke, and A. Neubauer. *Regularization of Inverse Problems.* Kluwer Academic Publishers, Dordrecht, the Netherlands, 1996.

[9] Xiao-Li Feng, Chu-Li Fu, and Hao Cheng. A regularization method for solving the cauchy problem for the helmholtz equation. *Applied Mathematical Modelling*, 35(7):3301 – 3315, 2011.

[10] G.J. Fix and S.P. Marin. Variational methods for underwater acoustic problems. *J. Comput. Phys.*, 28:253–270, 1978.

[11] P. C. Hansen. *Rank-Deficient and Discrete Ill-Posed Problems. Numerical Aspects of Linear Inversion.* Society for Industrial and Applied Mathematics, Philadelphia, 1997.

[12] Tomas Johansson. An iterative procedure for solving a Cauchy problem for second order elliptic equations. *Math. Nachr.*, 272:46–54, 2004.

[13] V.A. Kozlov and V.G. Maz'ya. Iterative procedures for solving ill-posed boundary value problems that preserve the differential equations. *Algebra i Analiz*, 1(5):144–170, 1989. translation in Leningrad Math. J. 1(1990), no. 5, pp. 1207–1228.

[14] V.A. Kozlov, V.G. Maz'ya, and A.V. Fomin. An iterative method for solving the cauchy problem for elliptic equations. *Comput. Maths. Math. Phys.*, 31(1):46–52, 1991.

[15] C. L. Lawson and R. J. Hanson. *Solving Least Squares Problems.* Prentice-Hall, Englewood Cliffs, NJ, 1974.

[16] L. Marin. Boundary element–minimal error method for the cauchy problem associated with helmholtz–type equations. *Comput. Mech.*, 44(2):205–219, 2009.

[17] L. Marin, L. Elliott, P. J. Heggs, D. B. Ingham, D. Lesnic, and X. Wen. An alternating iterative algorithm for the Cauchy problem associated to the Helmholtz equation. *Comput. Methods Appl. Mech. Engrg.*, 192(5-6):709–722, 2003.

[18] L. Marin, L. Elliott, P. J. Heggs, D. B. Ingham, D. Lesnic, and X. Wen. Conjugate gradient-boundary element solution to the Cauchy problem for Helmholtz-type equations. *Comput. Mech.*, 31(3-4):367–377, 2003.

[19] V. A. Morozov. On the solution of functional equations by the method of regularization. *Soviet. Math. Dokl.*, 7:414–417, 1966.

[20] F. Natterer. An initial value approach for inverse Helmholtz problems. Technical Report 19/96 N, Department of Mathematics, University of Münster, 1996.

[21] D.L. Phillips. A technique for the numerical solution of certain integral equations of the first kind. *J. Assoc. Comput.*, pages 84–97, 1962.

[22] H.H. Qin and T. Wei. Two regularization methods for the cauchy problems of the helmholtz equation. *Applied Mathematical Modelling*, 34:947–967, 2010.

[23] H.H. Qin, T. Wei, and R. Shi. Modified tikhonov regularization method for the cauchy problems of the helmholtz equation. *J. Comput. Appl. Math.*, 24:39–53, 2009.

[24] Teresa Regińska and Kazimierz Regiński. Approximate solution of a Cauchy problem for the Helmholtz equation. *Inverse Problems*, 22(3):975–989, 2006.

[25] Y Saad. *Iterative Methods for Sparse Linear Systems.* International Thomson Publishing, 1996.

[26] J.D. Shea, P. Kosmas, S.C. Hagness, and B.D. Van Veen. Three–dimensional microwave imaging of realistic numerical breast phantoms via a multiple–frequency inverse scattering technique. *Medical Physics*, 37(8):4210–4226, 2010.

[27] Y. Sun, D. Zhan, and F. M. A potential function method for the cauchy problem for elliptic operator. *J. Math. Anal. Appl.*, 395(1):164–174, 2012.

[28] A. N. Tikhonov. Solutions of incorrectly formulated problems and the regularization method. *Soviet Math. Dokl.*, 4:1035–1038, 1963.